Bound roton pairs in HeII under pressure: Analysis of Raman spectra

M. Shay, O. Pelleg, E. Polturak, and S. G. Lipson
Department of Physics, Technion–Israel Institute of Technology, Haifa 32000, Israel
(Received 29 August 2006; revised manuscript received 1 January 2007; published 21 February 2007)

We have investigated the properties of bound roton pairs in superfluid ^{4}He as a function of pressure using Raman scattering. Raman spectra at small energy shifts of 10–30 K were measured at several pressures up to the melting curve. The spectra reveal an asymmetric peak at about 2 times the energy of a roton, consistent with previous works. Our data, as well as previous measurements by Ohbayashi *et al.*, were analyzed according to a model for the two roton density of states. The value of the $l=2$ component of the interaction energy of a roton pair as a function of pressure was extracted from the analysis and compared with theoretical predictions. We find that this interaction changes sign from attractive to repulsive at pressure around 10 bar. The lifetime of a single roton as a function of temperature was also determined.

DOI: 10.1103/PhysRevB.75.054516 PACS number(s): 67.40.Db, 78.30.−j

Following Halley's suggestion,[1] the Raman spectrum of HeII was first measured by Greytak and Yan in 1969 (Ref. 2) and subsequently by others.[3–5] Soon after Greytak's experiment a theory to explain the spectrum was developed by several authors.[6–9] The observed asymmetric peak was interpreted as a result of a second order Raman scattering process in which the scattered photon loses energy to create two rotons. The spectrum therefore reflects the joint density of states of two rotons, and is influenced by roton-roton interaction. A model for the joint density of states at saturated vapor pressure (SVP) was constructed, in which interaction between rotons is attractive, so that roton pairs can form a bound state, and this bound state dominates the joint density of states.[8–11] According to the model, the Raman spectrum from superfluid helium contains information about the energy of the bound state E_b, the lifetime of a single roton γ^{-1}, and about Δ, the minimum energy of a roton. Raman spectra from superfluid helium up to the melting pressure were measured by Ohbayashi *et al.*[12,13] and also in the present work. Ohbayashi also analyzed the polarization of the Raman scattered light and found that scattering is due to pairs of rotons with $l=2$ total angular momentum. In this work we analyze new high pressure spectra and those from Ref. 13 according to the above model in order to extract the dependence of E_b and γ on pressure and temperature. We compare our results to a theoretical prediction by Bedell, Pines, and Zawadowski[14] (BPZ) that the two-roton bound state with angular momentum $l=2$ should exist only below 5 bar.

In Raman scattering from superfluid helium the Stokes spectrum is the result of a second order transition in which the incoming photon loses energy to create two elementary excitations with total momentum equal zero. In such a process, the line shape of the scattered light reflects the density of states of two elementary excitations with zero total momentum.[15] This can be seen if we compare the roton density of states to the Raman transition probability calculated using Fermi's golden rule. The joint density of states, ρ_2, is defined as

$$\rho_2(E) = \frac{1}{(2\pi)^3}\int d^3k\,\delta[E-2E(k)]. \tag{1}$$

The Raman transition probability density is given by Fermi's golden rule,

$$\frac{dP(E)}{dk_1} = \frac{2\pi}{\hbar}|\langle\mathcal{M}\rangle|^2\delta[E-E(k_1)-E(k_2)], \tag{2}$$

where $E=\hbar\omega_i-\hbar\omega_s$ and $\hbar\omega_i$, $\hbar\omega_s$ are the energies of the incident and scattered photon, k_1, k_2 are the wave vectors of elementary excitations, $E(k)$ is the dispersion relation, and $\mathcal{M}$ is the transition matrix. An integration over the set of final states yields the total transition probability. Fixing the direction of the scattered photon and its energy to a definite value $\hbar\omega_s$, the set of final states can be counted by integrating over k_1. k_2 is fixed by the condition of zero total momentum. Neglecting the momentum of the photons we get $k_1=-k_2$, $E(k_1)=E(k_2)$. Assuming the matrix element to be independent of k, the scattering probability can be written as

$$P(E) = \frac{2\pi}{\hbar}|\langle\mathcal{M}\rangle|^2\int\delta[E-2E(k)]d^3k = \frac{(2\pi)^4}{4\hbar}|\langle\mathcal{M}\rangle|^2\rho_2(E). \tag{3}$$

It is seen from Eq. (3) that the Raman scattering probability is proportional to the joint density of states times the square of the matrix element. The scattered photon can either change its polarization or not change its polarization. This restricts the angular momentum transfer to $l=0$ or $l=2$, while for all other cases the matrix element is zero. Polarization analysis of the Raman spectra of superfluid helium[11,12] shows that the scattering state is of angular momentum $l=2$ at all pressures. Therefore, the Raman scattering from superfluid helium is sensitive to the joint density of states of excitations with total momentum $K=0$ and angular momentum $l=2$. The density of states around the roton minimum in the dispersion relation is illustrated in Fig. 1. Figure 1(a) shows the density of states for the simplest model, that of noninteracting rotons. In this model a parabolic approximation is used for the dispersion relation around the roton minimum: $E(k)=\Delta+\frac{\hbar^2}{2\mu}(k-k_0)^2$, where Δ is the roton minimum energy, k_0 is the wave vector at the minimum and μ is the roton effective mass. Substituting this expression into Eq. (1), the joint density of states around the roton minimum at $T=0$ becomes[6,16]

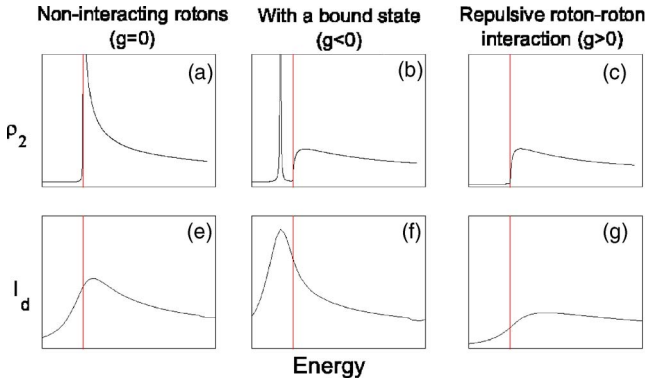

FIG. 1. (Color online) Upper panel, two-roton joint density of states with $K=0$ from Eq. (6) plotted for three situations: (a) Noninteracting rotons ($g=0$), (b) with a bound state ($g<0$), (c) with a repulsive roton-roton interaction ($g>0$). Lower panel (e)–(g), corresponding line shapes of the detected light intensity taking into consideration the instrumental resolution. The vertical line (red online) marks the position of 2Δ.

$$\rho_2(E) \propto (E-2\Delta)^{-1/2}\Theta(E-2\Delta). \tag{4}$$

It is interesting to note that Eq. (4) is similar to the density of states for a free particle in one dimension. Of course, the system is three dimensional and the 1D-like behavior can be traced to the finite value of k_0. The presence of roton-roton interaction changes $\rho_2(E)$ in a way which depends on the sign of the interaction. The density of states for the case of attractive interaction is shown in Fig. 1(b). An attractive interaction leads to a formation of a bound state with a binding energy E_b, adding a δ function at $2\Delta-E_b$ to Eq. (4). In addition, E_b is added to the denominator of Eq. (4), removing the divergence at 2Δ. If the interaction is repulsive, the density of states is shown in Fig. 1(c). In this case, there is no bound state and the δ function is not present. However, E_b in the denominator of Eq. (5) remains, representing the energy of the interaction. The coupling constant of the roton-roton interaction, g is related to E_b through $g^2 \propto E_b$. This model was used by Greytak *et al.*[10,11] to analyze their data at low (SVP) pressure. The density of states for the case of attractive interaction is given in Eq. (5),

$$\rho_2(E) \propto 2E_b^{1/2}\delta(E-2\Delta+E_b) + \frac{(E-2\Delta)^{1/2}}{(E-2\Delta+E_b)}\Theta(E-2\Delta). \tag{5}$$

Note that this model coincides with the free roton model when the binding energy is zero. At finite temperature, the density of states becomes

$$\rho_2(E) \propto k_0^2\mu^{1/2}\left[\frac{2\sqrt{E_b}\gamma}{(E-2\Delta+E_b)^2+\gamma^2} + \left(\frac{\sqrt{(E-2\Delta)^2+4\gamma^2}+(E-2\Delta)}{(E-2\Delta+E_b)^2+4\gamma^2}\right)^{1/2}\right]. \tag{6}$$

The temperature dependence of ρ_2 is through γ, the energy linewidth of the roton. Equation (6) coincides with that given by Zawadowski *et al.*,[9] based on the analysis of the two roton

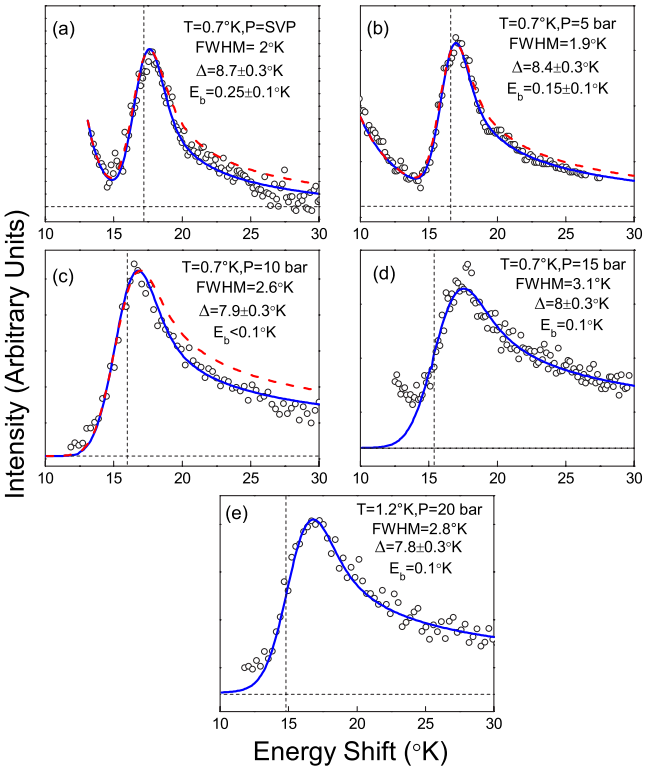

FIG. 2. (Color online) Raman spectra of HeII at different pressures. Solid lines (blue online) are fits to Eq. (6) taking into account instrumental broadening. The vertical dashed line marks the value of 2Δ taken from Ref. 17, and the horizontal dashed line marks the dark count level. The increasing background at low energy is the tail of the elastic peak. The dashed lines (red online) in panels (a) and (b) are fits to a model of noninteracting rotons. In panel (c) the dashed line is a fit with a small positive coupling constant. It shows that at 10 bar the interaction is still attractive.

Green's function (this was checked by plotting both formulas on the same graph). The comparison of Eq. (6) to the expression given by Zawadowski *et al.* [Eq. (3.24) from Ref. 9] shows that γ indeed represents the energy linewidth of a single roton. Because of the parabolic approximation to the dispersion relation in Eq. (6), the energy range where this equation is valid is limited. This range is between zero to about 2 times the energy of the maxon.

The measured intensity, I_d, is a convolution of the instrumental resolution function and the scattered intensity I_s,

$$I_d(E) = C\int R(E-\varepsilon)I_s(\varepsilon)d\varepsilon = C\int R(E-\varepsilon)\rho_2(\varepsilon)d\varepsilon, \tag{7}$$

where $R(E)$ is the instrumental resolution function. For a double grating monochromator this resolution function can be measured by scanning the elastically scattered light, since the energy linewidths of the Rayleigh and Brillouin scattering are much narrower than the resolution of the spectrometer. The fine structure of Eq. (6) is below the resolution of the double grating monochromator. The lower panel of Fig. 1 shows the effect of finite resolution on the line shape of the

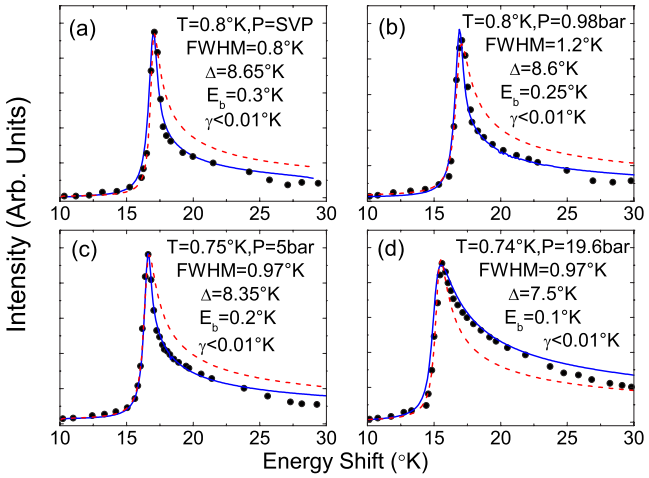

FIG. 3. (Color online) Raman spectra of HeII at different pressures from Ref. 13. The solid lines (blue online) are fits of Eq. (6) to the data. The dashed lines (red online) are a fit to a model of noninteracting rotons.

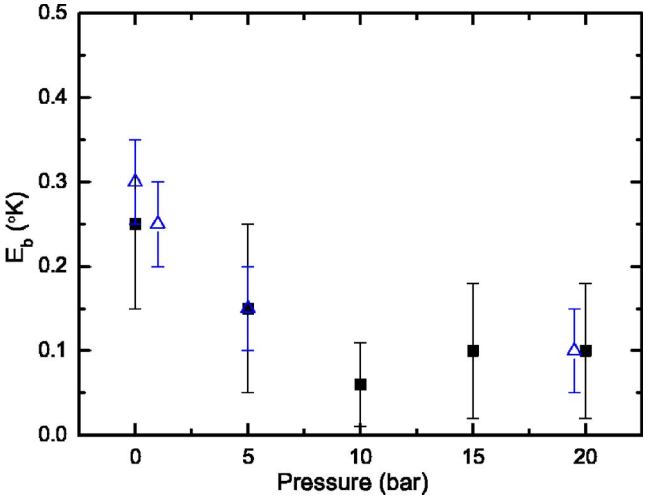

FIG. 4. (Color online) Pressure dependence of the binding energy from this experiment (black squares) and from the analysis of the experimental data from Ref. 13 [open triangles (blue online)]. Error bars are the uncertainty of the fit.

measured spectrum. We remark that the plots in Fig. 1 represent a high resolution system. Although the fine details of the density of states cannot be resolved due to finite resolution, there are clear differences in both the peak position and in the line shape of the spectra. The position at which the Raman peak is observed depends on resolution. This shift of the Raman peak towards higher energy at a lower spectrometer resolution is well known.[5] To be more specific, a Raman peak at an energy higher than 2Δ does not mean that there is no bound state. It is necessary to use the model convoluted with the resolution function in order to compare with experimental data.

In our experiment, a BeCu sample cell with three indium sealed windows is mounted on a ^{3}He refrigerator with optical access. The pressure in the cell is measured outside the cryostat using a high accuracy pressure gauge connected to the filling line. The cell temperature is measured using a calibrated germanium resistor. An argon ion laser beam is focused inside the sample cell. The intensity that enters the cell is 65 mW at 5145 Å. The beam exits the cryostat and is reflected back by a mirror to double the incident intensity. A chopper is used to reduce the heating of the cell caused by the laser beam. Using a duty cycle of 1:5, a steady temperature of 0.6 K could be achieved. The 90° scattered light is collected using a $f\#/8.5$ lens system that images the scattering volume onto the entrance slit of a computer controlled double grating spectrometer (Spex 1403) equipped with holographic gratings having 1800 grooves per mm. The image is aligned to the entrance slit using a Dove prism. A cooled photon counting photomultiplier with dark count of about 3 cps (Hamamatsu R6358P) converts the scattered light into electrical pulses. Each spectrum was scanned 10 times in intervals of 0.1 cm^{-1} between points. At every point the exposure time was 10 seconds so that the total exposure time at each point is 100 seconds. To determine the resolution function, the elastic peak was measured before each inelastic scan. In order to eliminate drifts, the wave number of each point is measured relative to the position of the elastic peak measured in the same scan.

Raman spectra from superfluid helium were obtained at several pressures from SVP to 20 bar. These spectra are shown in Fig. 2. We use Eqs. (6) and (7) to fit our experimental data with C, Δ, E_b, and γ as fitting parameters. The measured line shape at SVP [Fig. 2(a)] is reminiscent of Fig. 1(f). A prominent, rather symmetrical peak is observed. The width of the peak is limited by the resolution of the spectrometer. This line shape is characteristic of the existence of a bound state. On the other hand, the high pressure spectra [Figs. 2(d) and 2(e)], have line shapes that do not exhibit the bound state characteristics and are reminiscent of Fig. 1(g). The sensitivity of the line shape to the presence of the bound state can be clearly seen in Fig. 2(c). Here, the solid line is a fit with a bound state with a very small E_b, while the dashed line is a fit with the same E_b but a repulsive interaction. These observations immediately suggest that at elevated pressures the interaction changes from an attractive to repul-

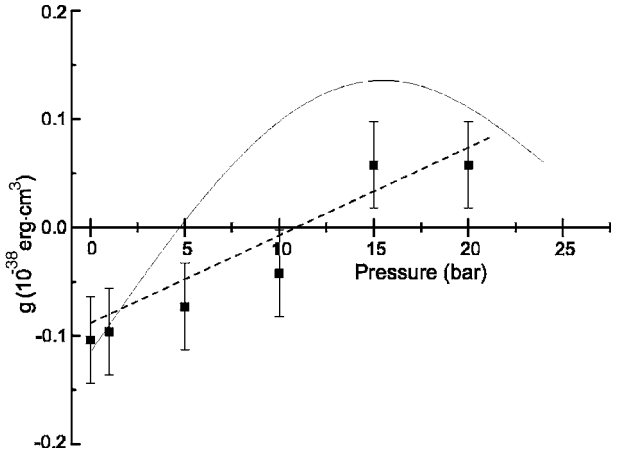

FIG. 5. Pressure dependence of the $l=2$ coupling constant. Black squares, extracted from Raman scattering data. The solid line is the prediction of BPZ. The dashed line represents calculations from Ref. 19, based on Raman scattering data.

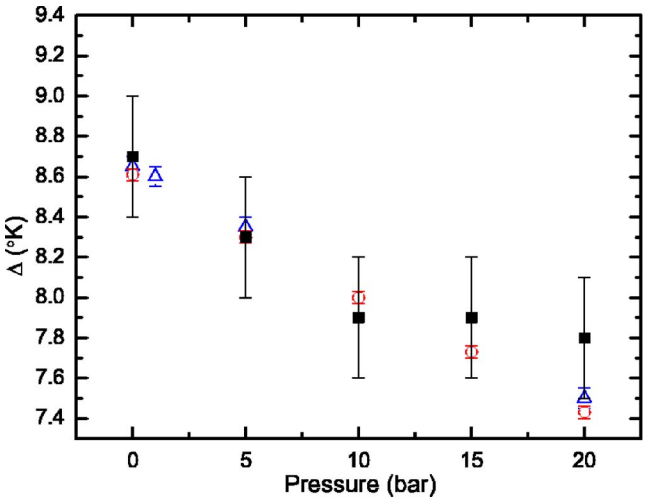

FIG. 6. (Color online) Pressure dependence of Δ from this experiment (black squares), from the analysis of the experimental data from Ref. 13 [open triangles (blue online)], and from neutron scattering data (Ref. 17) [open circles (red online)].

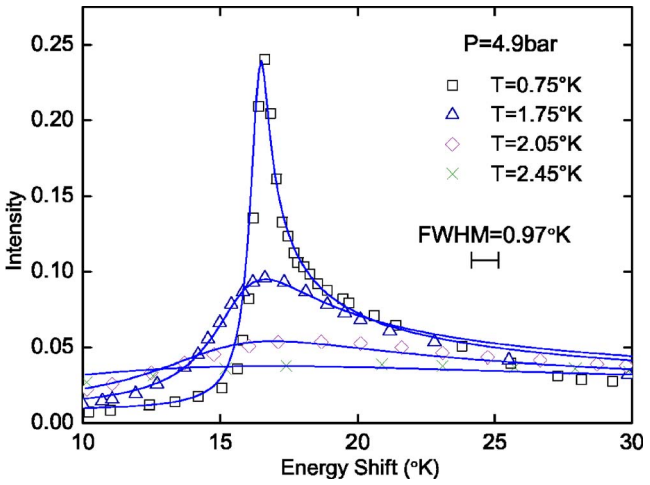

FIG. 7. (Color online) Fits of Eq. (6) to the Raman spectra at 4.9 bar. From Ref. 13. At this pressure a bound state still exists. The change of the spectrum induced by temperature is dominated by γ^{-1}, the lifetime of a single roton.

sive. In addition to our results, we also fit the high resolution data from Ref. 13. The fits are shown in Fig. 3. In this figure the solid line is a fit to the interacting roton model and the dashed line is the fit to the noninteracting model. It is evident that the interacting model fits the data well while the noninteracting model does not. The results of the fits of our data and that from Ref. 13 are consistent. The values of E_b as a function of pressure are shown in Fig. 4. We find that E_b decreases with pressure. At SVP $E_b=0.25\pm0.1$ K in agreement with previous works.[10,11] At a pressure of 10 bar E_b is at its lowest value of less than 0.1 K, and above 10 bar the data can only be fitted without a bound state. At these pressures E_b still has a small positive value which represents the interaction energy rather than the binding energy. Using the relation between E_b and the coupling constant g we plot in Fig. 5 the pressure dependence of g, and compare it to the theoretical prediction of BPZ. In addition, Nakajima and Namaizawa[19] proposed a different type of an interaction pseudopotential. In their work, the pseudopotential can either diverge or not, depending on the choice of the parameters. The values of g calculated for the nondivergent case are shown in Fig. 5 as the dashed line. Regarding the fitted values of Δ, these are in agreement with neutron scattering values (taken from Ref. 17) for all pressures, as shown in Fig. 6. We remark that the fit value of E_b is sensitive to both the peak position and the line shape of the Raman spectrum while the fit value of Δ is only influenced by the position of the Raman peak. Therefore, the analysis gives a tighter bound on E_b than on Δ.

We now turn to the analysis of the temperature dependence of the high resolution Raman spectra obtained by Ohbayashi *et al.*[13] The spectra which we analyze are at 4.9 bar and at four different temperatures between 0.75 K to 2.45 K. The original analysis[13] shows that the high temperature spectra are consistent with a convolution of the low temperature spectrum and a Lorenzian, and that the temperature dependence of the width of that Lorenzian is well described by the BPZ model. We have fitted Eq. (6) to the same data. The result is shown in Fig. 7. As mentioned, at this pressure the low temperature line shape is too narrow to be explained without a bound state. At 0.75 K the values of the fitting parameters are $E_b=0.2\pm0.05$ K, $\gamma<0.01$ K. Most of the temperature dependence of the spectra is due to the lifetime of a single roton. There is also a weak temperature dependence of k_0 and μ. With the values for k_0 and μ from Ref. 17, The constant C in Eq. (6) is indeed found to be temperature independent to within 5%. The use of the physical model expressed in Eq. (6) for the analysis enables us to extract the temperature dependence of γ, at the pressure of 4.9 bar. The values of γ, extracted from both the data of Ohbayashi *et al.* and from our data at 1.2 K, are in good agreement with the values obtained by Ohbayashi's analysis. In Fig. 8 we compare the measured temperature dependence of γ at 5 bar to

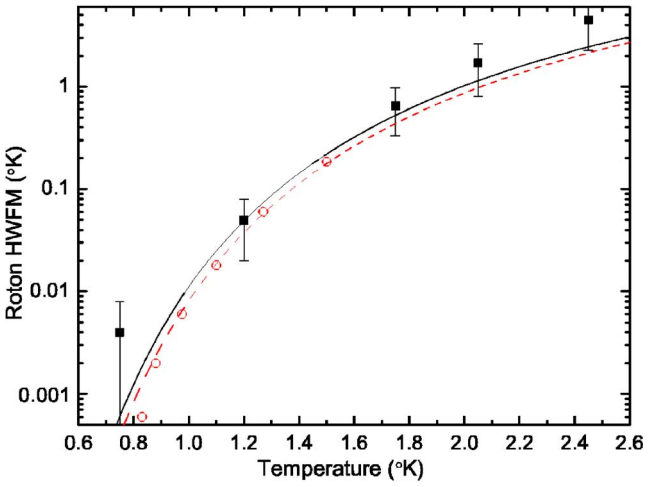

FIG. 8. (Color online) Temperature dependence of γ (black squares) at 5 bar extracted from Raman scattering data. The solid line is an approximation to the theoretical value given by BPZ at 5 bar. Values of γ measured by neutron scattering (Ref. 18) are shown as open circles (red online). The dashed line is the BPZ theory at SVP.

an approximation to the theoretical prediction of the BPZ model that is $\gamma(T)=42.3(1+0.0588T^{1/2})T^{1/2}\exp\left(\frac{\Delta(T)}{T}\right)$. The approximation that we use is $\Delta(T)=\Delta$. This approximation also worked well at SVP for neutron scattering data.[18] The neutron data and the BPZ prediction at SVP is also shown in the figure. The general trend predicted by the BPZ model, that the width increases with pressure is evident.

In conclusion, the Raman spectra of superfluid ^{4}He at several pressures were measured. The results are in agreement with previous experiments. The spectra are very well described by a model of interacting rotons presented by Ruvalds and Zawadowski[7,9] and Iwamoto[8] and developed by Bedell, Pines, and Zawadowski.[14] At SVP an $l=2$ bound state of two rotons exists with a binding energy of 0.3 ± 0.05 K. This bound state also exists at a pressure of 5 bar. Above 10 bar, the $l=2$ bound state seems to disappear yet the line shape is incompatible with the free rotons model. This observation suggests that the coupling constant of the $l=2$ component of the roton-roton interaction changes sign around 10 bar. Fitted values of the coupling constant are in a broad agreement with the pseudopotential theory presented by BPZ,[14] in the sense that the interaction changes sign at some pressure. The temperature dependence of the lifetime of a single roton is also in good agreement with the theory of BPZ. According to the models,[8,9] if the roton-roton interaction is repulsive a peak should appear in the spectrum at 2 times the maxon energy. However, existing experimental data shows no trace of such peak. The absence of such a peak when g is positive may suggest that the overall interaction between rotons remains attractive at high pressures, however it involves scattering via channels with $l>2$, which are not Raman active.

The authors thank E. Akkermans, A. Kanigel, and E. Farhi for useful discussions. The authors are grateful to S. Hoida, L. Iomin, and A. Post for technical support. The authors acknowledge the financial support of the Israel Science Foundation and of the Technion Fund for Research.

[1] J. W. Halley, Phys. Rev. **181**, 338 (1969).
[2] T. J. Greytak and J. Yan, Phys. Rev. Lett. **22**, 987 (1969).
[3] E. R. Pike and J. M. Vaughan, J. Phys. C **4**, L362 (1971).
[4] C. M. Surko and R. E. Slusher, Phys. Rev. Lett. **30**, 1111 (1973).
[5] K. Ohbayashi and M. Udagawa, Phys. Rev. B **31**, 1324 (1985).
[6] M. J. Stephen, Phys. Rev. **187**, 279 (1969).
[7] J. Ruvalds and A. Zawadowski, Phys. Rev. Lett. **25**, 333 (1970).
[8] F. Iwamoto, Prog. Theor. Phys. **44**, 1135 (1970).
[9] A. Zawadowski, J. Ruvalds, and J. Solana, Phys. Rev. A **5**, 399 (1972).
[10] T. J. Greytak, R. Woerner, J. Yan, and R. Benjamin, Phys. Rev. Lett. **25**, 1547 (1970).
[11] C. A. Murray, R. L. Woerner, and T. J. Greytak, J. Phys. C **8**, L90 (1975).
[12] M. Udagawa, H. Nakamura, M. Murakami, and K. Ohbayashi, Phys. Rev. B **34**, 1563 (1986).
[13] K. Ohbayashi, M. Udagawa, and N. Ogita, Phys. Rev. B **58**, 3351 (1998).
[14] K. Bedell, D. Pines, and A. Zawadowski, Phys. Rev. B **29**, 102 (1984).
[15] R. Loudon, Adv. Phys. **13**, 423 (1964).
[16] M. J. Stephen, in *The Physics of Liquid and Solid Helium*, edited by K. H. Bennemann and J. B. Ketterson (Wiley, New York, 1976), p. 307.
[17] M. R. Gibbs, K. H. Andersen, W. G. Stirling, and H. Schober, J. Phys.: Condens. Matter **11**, 603 (1999).
[18] K. H. Andersen, J. Bossy, J. C. Cook, O. G. Randl, and J. L. Ragazzoni, Phys. Rev. Lett. **77**, 4043 (1996).
[19] M. Nakajima and H. Namaizawa, J. Low Temp. Phys. **95**, 441 (1994).